Chemical Engineering Journal 163 (2010) 337–343

Contents lists available at ScienceDirect

Chemical Engineering Journal

journal homepage: www.elsevier.com/locate/cej

Single and binary biosorption of cerium and europium onto crab shell particles

K. Vijayaraghavan[a], R. Balasubramanian[b,*]

[a] Singapore-Delft Water Alliance, National University of Singapore, 2 Engineering Drive 2, Singapore 117577
[b] Division of Environmental Science and Engineering, National University of Singapore, Singapore 117576

ARTICLE INFO

Article history:
Received 13 March 2010
Received in revised form 1 August 2010
Accepted 3 August 2010

Keywords:
Rare earths
Crab shell
Isotherm
Kinetics
Multicomponent

ABSTRACT

The ability of crab shell to biosorb two rare earth elements (REE), namely cerium(III) and europium(III) from single and binary systems has been studied. Crab shell majorly comprised of calcium carbonate, protein and chitin. Experiments to identify the role of these constituents in REE biosorption revealed that calcium carbonate was mainly responsible for REE removal. Microprecipitation of REE by carbonate ions and subsequent settling on the surface of crab shell was identified as major mechanism responsible for crab shell biosorption performance. At optimum pH of 6, in single component system, crab shell exhibited maximum Ce(III) and Eu(III) uptakes of 144.9 and 49.5 mg/g, respectively, according to the Langmuir model. In binary systems, both Ce(III) and Eu(III) compete with each other resulted in decreased uptake. In an attempt to model the binary biosorption data, Sheindorf–Rebhun–Sheintuch equation provided more accurate prediction of isotherm data compared to extended Langmuir model with constant interaction factor. Kinetic experiments revealed that equilibrium was attained in 60 min, followed by complete saturation in 2 h, for both Ce(III) and Eu(III). Pseudo-first order model better predicted the kinetic data with high correlation coefficients and low % error values than pseudo-second order model.

1. Introduction

Rare earth elements (REEs) are widely used in metallurgy [1], ceramic industry [2], agriculture [3] and medicine [4] as well as in the nuclear industries [5]. Both radioactive and stable REEs can enter the food chain, resulting in their intake by humans. Considering the accumulation property of REEs and its relative toxicity towards living organisms [6,7], there is a need to find a suitable and economical treatment method for REE-bearing solutions.

In recent years, adsorption using biological materials has been identified as a potential method for the remediation of metal-bearing solutions. Biosorbents for the removal of metal ions mainly come under the following categories: bacteria, fungi, algae, industrial waste, agricultural wastes and other polysaccharide materials. In general, all types of biomaterials have shown good biosorption capacities towards all types of metal ions. The inherent advantages and applications of biosorption have been extensively reviewed by several investigators [8,9]. Of the different types of biosorbents, macroscopic and industrial/agricultural wastes are generally preferred for successful biosorption processes. Microbial biosorbents are basically small particles with low density, poor mechanical strength and little rigidity. Even though they excel with high biosorption capacity, they suffer with solid–liquid separation, biomass swelling, impossibility of regeneration/reuse and development of a high pressure drop when used in continuous column mode [9]. Researchers also identified biosorbents which showed good mechanical stability as well as good biosorption ability [9,10]. One such biosorbent is crab shell waste, obtained from seafood industries. Due to its high calcium carbonate, chitin and protein contents, crab shell performed well in sorption of several heavy metal ions and metalloids, including lead [11], cadmium [12], chromium [13], copper [14], cobalt [14], nickel [15], zinc [16] and arsenic [17]. A very good mechanical stability and ease in desorption enabled the biosorbent to be reused and regenerated up to 5 cycles [15].

Cerium and europium were used as model solutes in the present study. Both are abundant and widely employed in many industrial applications [18,19]. Despite their strategic and economical importance, these REEs have not been extensively studied for biosorption processes. Of the limited literatures, Diniz and Volesky [20] investigated the ability of *Sargassum polycystum* to bind lanthanum, europium and ytterbium from single and multicomponent batch systems. The metal affinity sequence established was Eu > La > Yb. Also, Sert et al. [21] demonstrated that lanthanum and cerium can be recovered from single component synthetic solutions using *Platanus orientalis* leaf powder.

This study focuses on exploring the biosorption potential in the recovery of cerium and europium using crab shell particles in single and binary REE systems. In addition, the mechanism and the components associated with removal of REE will be studied.

---

[*] Corresponding author. Tel.: +65 65165135; fax: +65 67744202.
E-mail address: eserbala@nus.edu.sg (R. Balasubramanian).

1385-8947/$ – see front matter © 2010 Elsevier B.V. All rights reserved.
doi:10.1016/j.cej.2010.08.012

2. Materials and methods

2.1. Sorbent preparation

Waste shells of *Portunus sanguinolentus*, commonly known as three spot crabs, were collected from Marina beach, Chennai, India. The shells were washed extensively with deionized water and sun dried. The dried shells were crushed to particle sizes in the range of 0.5–1 mm. The shell particles were then treated with 0.1 M HCl at solid–liquid ratio of 10 g/L for 4 h followed by washing several times with deionized water and then dried in an oven at 60 °C overnight. This pre-treatment process was carried out to ensure the removal of excess calcium carbonate on the shell surface [22]. The pre-treated crab shell particles will be designated as "CSP" from now on in this paper. To elucidate the components responsible for REE removal, CSP was further exposed to 1N HCl for 6 h to completely remove mineral (calcium, sodium, potassium, zinc and magnesium) constituents [23] of crab shell particles [24]. The residue (mainly protein and chitin) was washed extensively with deionized water and dried at 60 °C overnight. The product obtained was designated as "DMCSP". To produce chitin, DMCSP was further exposed to 1 M NaOH at 100 °C for 3 h to remove protein. After reaction period, the residue was filtered and washed with deionized water to neutral.

2.2. Biosorption experimental procedure

Biosorption experiments were performed in a 250 mL Erlenmeyer flasks containing desired concentration of 100 mL REE solutions adjusted to desired pH using 0.1 M HCl or NaOH. A known quantity of biosorbent (0.5 g) was added to each flask, and agitated at 23 ± 2 °C in a 160 rpm rotary shaker. For binary systems, the REE concentration ratio was always maintained at 1:1 (in weight basis). During the binary isotherm study, initial total REE concentrations varied from 200 to 2000 mg/L. The pH of the reaction mixture was controlled at the desired value by the addition of 0.1 M HCl or NaOH during the experiments. After 8 h, the reaction mixture was filtered through a 0.45 μm PTFE membrane filter and analyzed for Ce and Eu concentrations using inductively coupled plasma-atomic emission spectrometer (ICP-AES; Perkin Elmer Optima 3000 DV). Kinetic experiments were conducted using the same method as above, except that the samples were collected at different time intervals to determine the time point at which biosorption equilibrium was attained.

The amount of REE sorbed by biosorbent was calculated from the differences between the REE quantity added to the biosorbent and the REE content of the supernatant using the following equation:

$$Q = \frac{V(C_0 - C_f)}{M} \tag{1}$$

where Q is the REE uptake (mg/g); C_0 and C_f are the initial and equilibrium REE concentrations in the solution (mg/L), respectively; V is the solution volume (L); and M is the mass of biosorbent (g).

2.3. Models to fit biosorption isotherms and kinetics

Four equilibrium isotherm models were used to fit the single component experimental data, as follows:

Langmuir model [25]:

$$Q = \frac{Q_{\max}\ bC_f}{1 + bC_f} \tag{2}$$

Freundlich model [26]:

$$Q = K_F C_f^{1/n} \tag{3}$$

Redlich–Peterson model [27]:

$$Q_e = \frac{K_{RP} C_f}{1 + a_{RP} C_f^{\beta_{RP}}} \tag{4}$$

Sips model [28]:

$$Q_e = \frac{K_S C_f^{\beta_S}}{1 + a_S C_f^{\beta_S}} \tag{5}$$

where $Q_{\max}$ is the maximum REE uptake (mg/g), b is the Langmuir equilibrium constant (L/mg), K_F is the Freundlich constant (mg/g) $(\mathrm{L/mg})^{1/n}$, n is the Freundlich constant, K_{RP} is the Redlich–Peterson isotherm coefficient (L/g), a_{RP} is the Redlich–Peterson isotherm coefficient $(\mathrm{L/mg})_{RP}^{\beta}$, β_{RP} is the Redlich–Peterson model exponent, K_S is the Sips model isotherm coefficient $(\mathrm{L/g})_s^{\beta}$, a_S is the Sips model coefficient $(\mathrm{L/mg})_s^{\beta}$ and β_S is the Sips model exponent.

The binary biosorption isotherms were described using an extended Langmuir equation, with a constant interaction factor [29], which can be represented for binary mixtures, as follows:

$$Q_1 = \frac{Q_{\max 1} b_1 (C_1/\eta_1)}{1 + b_1(C_1/\eta_1) + b_2(C_2/\eta_2)} \tag{6}$$

$$Q_2 = \frac{Q_{\max 2} b_2 (C_2/\eta_2)}{1 + b_1(C_1/\eta_1) + b_2(C_2/\eta_2)} \tag{7}$$

where $Q_{\max1}$, $Q_{\max2}$, b_1 and b_2 are the single component Langmuir parameters for the first (Ce) and second (Eu) REEs. Interaction factors, η_1 and η_2 are for the first and second REE, respectively. The calculation of the interaction factor is based on minimizing the following error function [30]:

$$\frac{100}{n-p} \sum_{i=1}^{n} \left[\frac{(Q_{e,\text{meas}} - Q_{e,\text{cal}})^2}{Q_{e,\text{meas}}} \right]_i \tag{8}$$

where n and p are the number of data points and parameters, respectively.

Also, the Sheindorf–Rebhun–Sheintuch (SRS) equation [31] was employed in the present study, which can be represented for binary mixtures as follows [32]:

$$(Q)_i^j = K_{F_i} C_{f_i} [C_{f_i} + \theta_{ij} C_{f_i}]^{[(1/n_i)-1]} \tag{9}$$

where $(Q)_i^j$ is the amount of solute, i, sorbed per unit weight of CSP in the presence of solute, j, K_{F_i} is the single component Freundlich constant for solute i, n_i is the Freundlich exponent for solute i and θ_{ij} is the competitive coefficient.

The experimental biosorption kinetic data were modeled using pseudo-first and -second order kinetics, which can be expressed in their non-linear forms, as follows:

Pseudo-first order model [33]:

$$Q_t = Q_e(1 - \exp(-k_1 t)) \tag{10}$$

Pseudo-second order model [34]:

$$Q_t = \frac{Q_e^2 k_2 t}{1 + Q_e k_2 t} \tag{11}$$

where Q_e is the amount of REE sorbed at equilibrium (mg/g), Q_t is the amount of REE sorbed at time t (mg/g), k_1 is the pseudo-first order rate constant (1/min) and k_2 is the pseudo-second order rate constant (g/mg min). All the model parameters were evaluated by non-linear regression using Sigma Plot (version 4.0, SPSS, USA) software. The average percentage error between the experimental and predicted values is calculated using:

$$\varepsilon(\%) = \frac{\sum_{i=1}^{N} (Q_{\exp,i} - Q_{\text{cal},i})/Q_{\exp,i}}{N} \times 100 \tag{12}$$

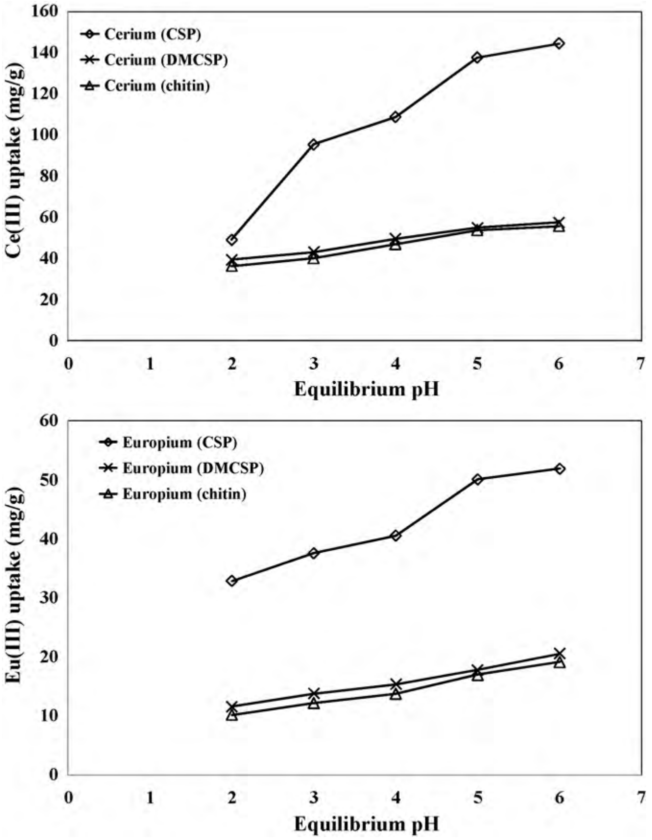

Fig. 1. Effect of equilibrium solution pH on the biosorption of Ce(III) and Eu(III) from single component systems by CSP, DMCSP and chitin (conditions: initial REE concentration = 998 mg/L; biosorbent dosage = 5 g/L; agitation rate = 160 rpm).

where Q_{exp} and Q_{cal} represents experimental and calculated REE uptake values, respectively, and N is the number of measurements. All experiments were done in duplicates and the data are the average values of two experiments.

3. Results and discussion

3.1. Effect of pH on REE biosorption

The solution pH is one of the dominant parameters controlling biosorption. Ce(III) and Eu(III) biosorption onto CSP as a function of pH ranging from 2 to 6 are given in Fig. 1. The removal of both Ce(III) and Eu(III) by CSP was highly dependent on pH. The biosorption of Ce(III) increased from 49.2 mg/g (pH 2) to 144.4 mg/g (pH 6), whereas Eu(III) increased from 32.9 mg/g (pH 2) to 52 mg/g (pH 6). The crab shell comprises mainly calcium carbonate and chitin along with some proteins [14,35]. Calcium carbonate in CSP favors microprecipitation of REE as $CaCO_3$ dissociates to Ca^{2+} and $CO_3{}^{2-}$. Also there was a rapid raise in solution pH when CSP was contacted with both Ce(III) and Eu(III) solutions. For instance, the initial pH 6 was increased to 8.3 within 20 min of contact. This is due to the following reaction:

$$\mathrm{Crabshell}(CaCO_3, \mathrm{chitin, protein}) + H_2O \rightarrow \mathrm{crabshell}\ (\mathrm{chitin, protein}) + Ca^{2+} + CO_3{}^{2-} \quad (13)$$

$$CO_3{}^{2-} + H_2O \rightarrow HCO_3{}^{-} + OH^{-} \quad (14)$$

The solubility of $CaCO_3$ may vary with the solution pH. The speciation of carbonate ions can be defined in three pH ranges, $pK_1 = 6.3$ and $pK_2 = 10.3$ [36]. Therefore, H_2CO_3, $HCO_3{}^{-}$ and $CO_3{}^{2-}$ species predominate for $pH < pK_1$, $pK_1 < pH < pK_2$, and $pH > pK_2$, respectively [37]. Among these carbonate species, $HCO_3{}^{-}$ and $CO_3{}^{2-}$ could be responsible for the formation of insoluble REE carbonates.

The hydrochemical behavior of REE is strongly influenced by their solution speciation [38]. At acidic pH values (pH < 5), lanthanides (Ln) exist in their trivalent form [39]. Under these pH conditions, initial hydroxide concentration was negligible and hence the concentration of $LnOH^{+}$ was minimal. Considering this observation, the formation of $LnCO_3{}^{+}$ and $Ln(CO_3)_2{}^{-}$ is more likely to occur at these high carbonate concentrations from CSP [40].

$$Ln^{3+} + CO_3{}^{2-} \rightarrow LnCO_3{}^{+} \quad (15)$$

$$Ln^{3+} + 2CO_3{}^{2-} \rightarrow Ln(CO_3)_2{}^{-} \quad (16)$$

$$Ln^{3+} + 2HCO_3{}^{-} \rightarrow Ln(CO_3)_2{}^{-} + 2H^{+} \quad (17)$$

Pourret et al. [40] illustrated that the formation of $LnCO_3{}^{+}$ and $Ln(CO_3)_2{}^{-}$ strongly depends on the pH and carbonate content. $LnCO_3{}^{+}$ concentrations decrease with pH increase, whereas $Ln(CO_3)_2{}^{-}$ concentrations increase when pH increases. At weak acidic values, the formation of $LnCO_3{}^{+}$ is more favorable [40]. This species is likely to form strong $Ln_2(CO_3)_3$ precipitates, which were then adsorbed to the chitinous material (chitin, protein and some minerals) present on the surface of CSP. At low pH values, the H_2CO_3 tends to dominate and theoretically Ln^{3+} cannot react with carbonate, which therefore resulted in decreased REE biosorption.

In order to confirm the importance of calcium carbonate in REE biosorption, CSP was subjected to various chemical treatments. The REE biosorption performance of CSP was compared with DMCSP and chitin as shown in Fig. 1. After removal of $CaCO_3$ from CSP, the maximum REE removal efficiencies decreased drastically. The DMCSP which comprises mainly of chitin and protein took only 57.6 and 20.6 mg/g of Ce(III) and Eu(III), respectively, at pH 6. Further removal of protein from DMCSP resulted in chitin, which performed almost identical to that of DMCSP in REE removal. Chitin, a straight-chain polymer composed of β-1,4-N-acetylglucosamin, is a known metal sorbent [41]. In chitin, hydroxyl and acetamido groups are prevalent; in particular, acetamido group of chitin acts as a non-specific chelator and establishes weak hydrogen bonds with REE in solution. However, the performance of chitin on the removal of Ce(III) and Eu(III) was only mediocre compared to the performance of CSP. Thus, it can be inferred that $CaCO_3$ is the main component responsible for the biosorption of REE by crab shell.

It is often useful to study the sorption behavior of a material when there is more than one component in the solution, e.g., to test a material in "more real" feed conditions. Thus, efforts were made to study the performance of CSP in binary REE system. As shown in Fig. 2, CSP performed well in the case of Ce(III) compared to Eu(III). However, while comparing the single-solute systems, the removal efficiencies of CSP decreased significantly. This is possibly due to competition between two REES for carbonate ions from CSP. Similar to single component systems, the REE removal efficiency increased with increase in solution pH and maximum total biosorptional uptake was observed at pH 6.

3.2. Single component Isotherms and modeling

Next, experiments were conducted to evaluate the full saturation capacity of CSP. Experimental single component biosorption isotherms at two different pH conditions are presented in Fig. 3. CSP exhibited high Ce(III) and Eu(III) uptakes at pH 6, in the order of magnitude of 2.9 and 1.6 times higher for Ce(III) and Eu(III), respectively, compared correspondingly with pH 2. Among the two REEs, CSP biosorbed more Ce(III) than Eu(III). For instance, at pH 6, CSP biosorbed 144.4 mg Ce(III)/g compared to 52 mg Eu(III)/g.

Single component biosorption isotherms were modeled using the Langmuir, Freundlich, Redlich–Peterson and Sips equations.

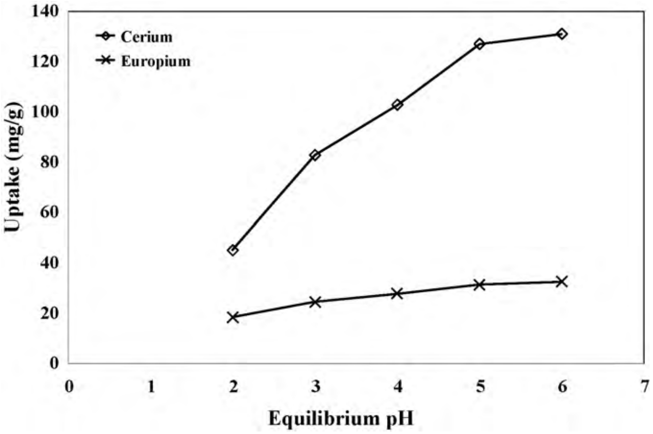

Fig. 2. Effect of equilibrium solution pH on the biosorption of Ce(III) and Eu(III) from binary systems by CSP (conditions: initial Ce(III) concentration = 996 mg/L; initial Eu(III) concentration = 1000 mg/L; biosorbent dosage = 5 g/L; agitation rate = 160 rpm).

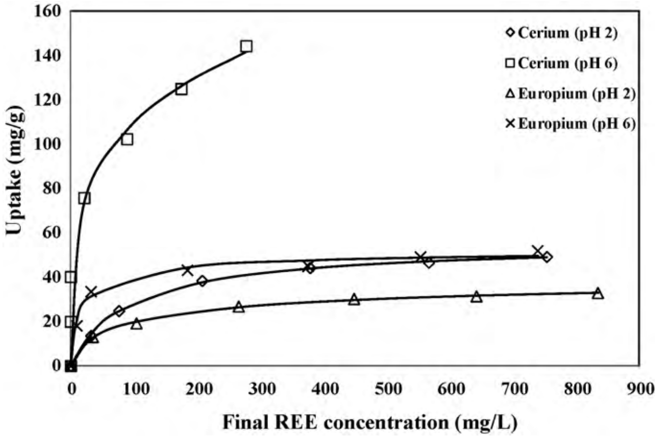

Fig. 3. Single component biosorption isotherms at different pH conditions (conditions: biosorbent dosage = 5 g/L; agitation rate = 160 rpm). Curves were predicted by the Sips model.

The model constants, along with correlation coefficients (R^2) and % error values obtained from four isotherm models are presented in Table 1. The Langmuir model served to estimate the maximum uptake values (Q_{max}) when these could not be experimentally obtained. The constant b represents the affinity between the sorbent and sorbate. For both Ce(III) and Eu(III), high Q_{max} and b values were observed at pH 6. The biosorption capacities observed for Ce(III) and Eu(III) in the present study were superior to the results published in the literature. The leaf powders of *Platanus orientalis* exhibited 32.1 mg Ce(III)/g [21] and *Pinus brutia* exhibited 17.2 mg Ce(III)/g [42] compared to 144.9 mg Ce(III)/g by CSP in this study. In Eu(III) biosorption, *Mycobacterium smegmatis* exhibited 19.1 mg/g [43] and *Pseudomonas aeruginosa* showed 44.1 mg/g [44] and compared to 49.5 mg/g by CSP in this study.

The relationship between the REE uptake capacity (Q) of CSP and the residual REE concentration (C_f) at equilibrium can also be described using the Freundlich equation. From Table 1, it was obvious that maximum K_F and n values were obtained at pH 6. High K_F and n values indicate that the binding capacity has reached its highest value; and the affinity between the biosorbent and REE was also higher. The experimental n values were greater than unity in all cases, indicating favorable biosorption [45]. The Redlich–Peterson model incorporates the features of both the Langmuir and the Freundlich isotherms into a single equation. There are two limiting behaviors: the Langmuir form for $\beta_{RP} = 1$ and the Henry's law form for $\beta_{RP} = 0$. The isotherm constants (K_{RP} and a_{RP}) and model exponent (β_{RP}) were recorded maximum at pH 6. Another, three-parameter model (Sips model) was also used to describe the REE isotherm data. At low sorbate concentrations, Sips isotherm effectively reduces to the Freundlich isotherm. At high sorbate concentrations, it predicts a monolayer sorption capacity characteristic of the Langmuir model. The isotherm constants were observed maximum at pH 6 for both Ce(III) and Eu(III). The exponent β_S values were generally observed close to unity, except for Ce(III) at pH 6 (Table 1).

In general, for single component isotherm data, all the examined isotherm models were able to simulate the experimental data with very good accuracy. In particular, both three-parameter models produced satisfactory simulation with high correlation coefficients and very low % error values.

3.3. Binary biosorption isotherms

Experimental data of binary biosorption system of Ce(III) and Eu(III) at different pH conditions are shown in Fig. 4. Comparing the two REEs, the Ce(III) biosorption isotherm is "L" shaped without strict plateau [46]. To be precise, the ratio between the concentration of Ce(III) remained in solution and sorbed on the

Table 1
Single component isotherm model parameters.

Models		Cerium		Europium	
		pH 2	pH 6	pH 2	pH 6
Langmuir	Q_{max} (mg/g)	55.1	144.9	34.99	49.53
	b (L/mg)	0.011	0.043	0.014	0.062
	R^2	0.999	0.957	0.999	0.997
	ε (%)	0.89	33.5	1.01	1.03
Freundlich	K_F (mg/g) (L/mg)$^{1/n}$	5.85	33.37	5.46	15.23
	n	3.03	3.89	3.66	5.34
	R^2	0.993	0.963	0.998	0.995
	ε (%)	3.95	33.4	1.01	2.16
Redlich–Peterson	K_{RP} (L/g)	1.21	18.73	0.76	4.54
	a_{RP} (L/mg)$^{\beta}_{RP}$	0.0089	0.39	0.0512	0.147
	β_{RP}	0.876	0.899	0.8745	0.924
	R^2	0.999	0.962	0.999	0.998
	ε (%)	0.19	32.6	0.12	0.56
Sips	K_S (L/g)$^{\beta}_{s}$	0.684	33.06	1.65	6.36
	a_S (L/mg)$^{\beta}_{s}$	0.0122	0.025	0.0393	0.119
	β_S	0.961	0.279	0.674	0.714
	R^2	0.999	0.963	0.999	0.998
	ε (%)	0.62	33.4	0.07	0.66

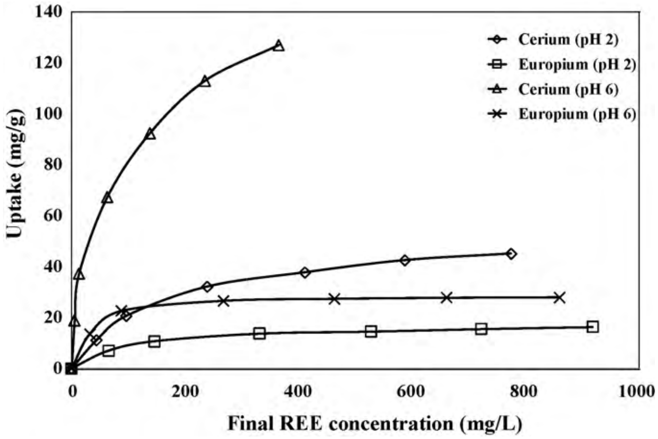

Fig. 4. Binary biosorption isotherms at different pH conditions (Conditions: biosorbent dosage = 5 g/L; agitation rate = 160 rpm).

solid decreases when the Ce(III) concentration increases, providing a concave curve. On the other hand, the Eu(III) biosorption isotherm at pH 6 is approximately "H" shaped [46]. It is one particular case of "L" shaped isotherm, where the initial slope is very high. This implies the high affinity of Eu(III) to the sorbent. However, as the concentration increases Ce(III) formed carbonates easily than Eu(III) as explained very well by the high Ce(III) uptakes at high concentrations. At pH 2, despite of decreased biosorption capacity, same trend of competition was observed. In order to quantify the competitive effect, the selectivity factor (β) of REEs was used and can be defined by [47]:

$$\beta_{1/2} = \frac{q_{eq1}/q_{eq2}}{C_{0,1}/C_{0,2}} \qquad (18)$$

where subscripts "1" and "2" represents Ce(III) and Eu(III), respectively; q_{eq} and C_0 represents REE uptake and initial REE concentration, respectively. The selectivity factor is useful to understand the preference of a sorbent towards a particular solute in a multi-solute system and the possibility of selective separation of particular solute. Clearly, β for Ce(III)/Eu(III) system increases with increasing their corresponding initial concentrations. This indicates the influence of Ce(III) towards the carbonate ions of CSP. The selectivity factor increased from 1.4 to 4.5 (pH 6) and 1.6 to 2.8 (pH 2) as the initial concentration increased from 100 to 1000 mg/L. This result supports the fact that at low solute concentrations there were adequate carbonate ions for the precipitation process. However, as the solute concentration increases, Ce(III) competed well and reacted with more carbonate ions.

Due to the competition between two REEs, the performance of CSP in binary systems was significantly affected. On comparing the binary biosorption system with the single component system for the highest REE uptake, the decrease was 12 and 46.2% for Ce(III) and Eu(III), respectively, at pH 6. This decrease was 8.1 and 50.2% for Ce(III) and Eu(III), respectively, at pH 2.

3.4. Binary biosorption modeling

In the present study an extended Langmuir equation, with a constant interaction factor, was used to describe the binary isotherm data. The conventional extended Langmuir equation assumes no interaction between solutes; which is not valid in real conditions [30]. To incorporate solute–solute interactions and competitions, an interaction factor (η) has been introduced into the extended Langmuir equation [29]. In the present study, η was assumed to be constant and specific for each solute in the binary systems, and the values are listed in Table 2. However, the model, in most cases, was unable to describe binary isotherms resulted in poor correlation coefficients and very high % error values. The reason for this discrepancy may be due to competition and interaction between the REEs, which was very significant; and the saturation capacity of each REE in single-solute systems was also different [30]. It should be noted that single component Langmuir isotherm model constants were used to model the binary biosorption data, as described in Section 2.3. Also, the interaction factor, η, does not have a strong theoretical foundation, with several investigators having employed the model with only limited success [30,48].

Table 2
Binary isotherm model parameters.

Models		pH 2	pH 6
Extended Langmuir equation	η_1	0.69	0.41
	η_2	1.91	5.01
	R_1^2	0.814	0.914
	R_2^2	0.837	0.747
	ε_1	21.3	47.6
	ε_2	33.5	35.4
SRS equation	θ_{12}	0.17	0.12
	θ_{21}	2.28	3.3
	R_1^2	0.978	0.987
	R_2^2	0.987	0.934
	ε_1	10.2	15.9
	ε_2	2.2	10.1

To improve the fitness, the SRS equation, which is a multicomponent Freundlich type equation, was used to describe the binary isotherm data. The model comprised of a competitive coefficient (θ_{ij}), which is based on the assumption that there is an exponential distribution of adsorption energies available for each solute. Interestingly, the model was able to predict the binary biosorption isotherm with relative success using the single component parameters. High correlation coefficients and low % error values, within the ranges of 0.934–0.987 and 2.2–15.9%, respectively, were obtained. As already proved in our experiments, that the magnitude of Ce(III) competition over Eu(III) was significant, and this data got confirmed by the SRS equation yielding high competitive coefficients for Eu(III) over Ce(III) (Table 2). The accuracy of fitness by the SRS equation to the binary REE system was represented in a three-dimensional plot as shown in Fig. 5. Here, the experimental results are shown by discrete points and the model prediction by the mesh surface. As shown in Fig. 5, the SRS equation exhibits excellent reproduction of the experimental data at the whole concentration range.

3.5. Kinetic studies

The biosorption kinetics of Ce(III) and Eu(III) onto CSP at different initial REE concentrations was studied. Fig. 6 illustrates the amount of REE sorbed onto CSP as a function of time. A close examination of the curves reveals that 96% removal efficiency was observed within 60 min for Ce(III) and 85 min for Eu(III). This initial quick phase was followed by slow attainment of equilibrium as high amount of carbonate were initially available for microprecipitation of REE, but thereafter, the formation of REE carbonate would be difficult due to decrease in carbonate release from the CSP. On changing the initial REE concentration from 250 to 1000 mg/L, the uptake increased from 50.1 to 144 mg/g for Ce(III) and 36.2 to 52.4 mg/g for Eu(III). In contrary, the corresponding removal efficiencies decreased from 97.9 to 85.6% for Ce(III) and 85.5 to 26.1% for Eu(III), while increasing the concentration from 250 to 1000 mg/L. This difference can be attributed to the fact that the ratio of the initial moles of REE to the available moles of calcium carbonate on the crab shell surface was low and subsequently the fractional sorption became independent of initial concentration of REE. However, at higher concentrations the available moles of cal-

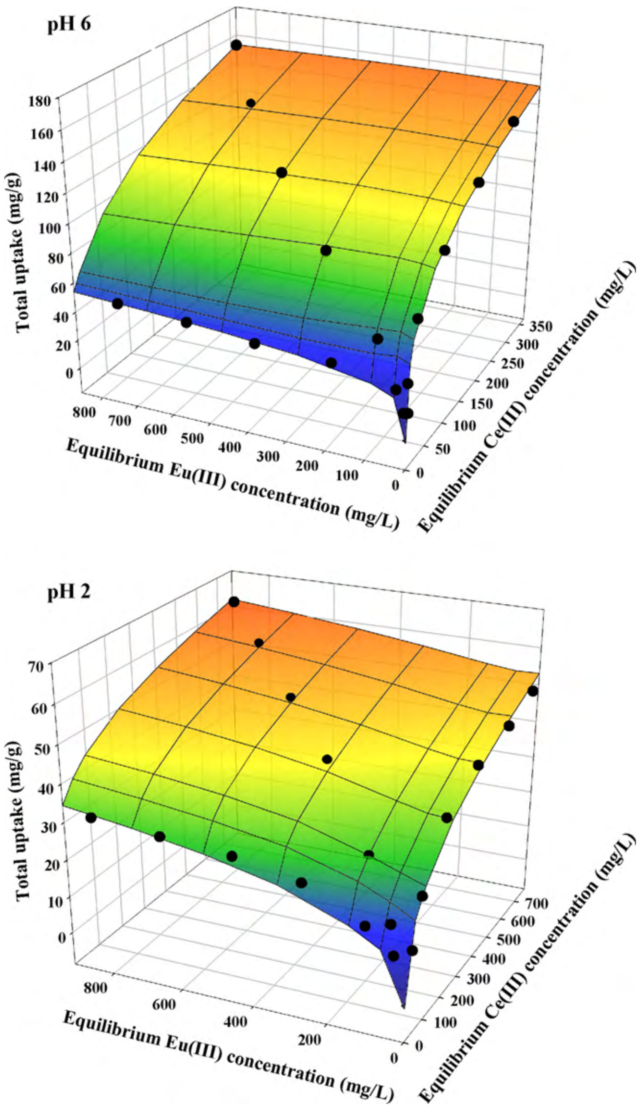

Fig. 5. Total REE uptake as the function of the equilibrium concentration in the Ce(III)–Eu(III) binary biosorption system (conditions: biosorbent dosage = 5 g/L; agitation rate = 160 rpm). Mesh surface predicted by the SRS equation.

cium carbonate become less compared to the moles of REE present. Hence, the percentage removal efficiency is dependent upon the initial solute concentration.

The experimental kinetic data were modeled using the pseudo-first and -second order kinetics. The model rate constants, predicted equilibrium REE uptakes, along with correlation coefficients and % error values are presented in Table 3. The pseudo-first order model successfully predicted the equilibrium uptake values with low % error values. On the other hand, the pseudo-second order model over predicted the Q_e values and also resulted in high % error values compared to pseudo-first order model. The curves predicted by the pseudo-first order model for biosorption kinetics data at different initial REE concentrations are shown in Fig. 6.

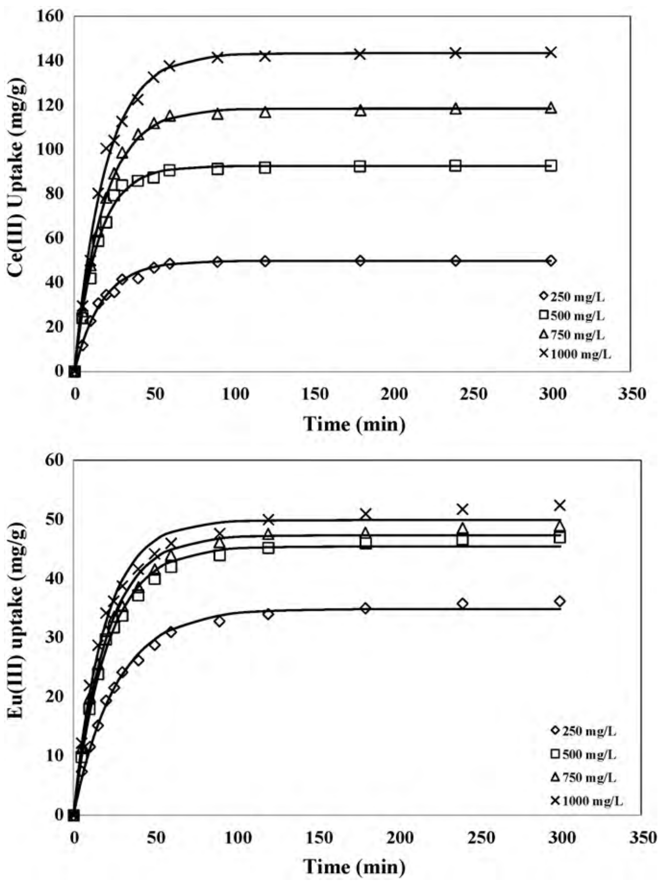

Fig. 6. Biosorption kinetic plots at different initial REE concentrations (Conditions: pH = 6; biosorbent dosage = 5 g/L; agitation rate = 160 rpm). Curves were predicted by pseudo-first order model.

4. Conclusions

From the present study, the following conclusions can be made:

- Crab shell was identified as a potent biosorbent for the removal of Ce(III) and Eu(III) from single and binary systems.
- An examination on the role of calcium carbonate, protein and chitin revealed that calcium carbonate was mainly responsible for REE biosorption through microprecipitation of REE ions onto the surface of crab shell.
- At optimum pH of 6, crab shell exhibited maximum Ce(III) and Eu(III) uptakes of 144.9 and 49.5 mg/g, according to the Langmuir model.

Table 3
Kinetic model parameters at different initial REE concentrations.

REEs	Initial concentration (mg/L)	$(Q_e)_{exp}$ (mg/g)	Pseudo-first order model				Pseudo-second order model			
			k_1 (1/min)	Q_e (mg/g)	R^2	ε (%)	k_2 (g/mg min)	Q_e (mg/g)	R^2	ε (%)
Ce(III)	250	50.1	0.058	49.7	0.999	0.04	0.0015	54.8	0.998	2.41
	500	92.8	0.067	92.6	0.999	0.96	0.0009	101.5	0.995	3.10
	750	118.8	0.054	118.5	0.999	0.66	0.0006	131.3	0.996	3.08
	1000	144.0	0.052	143.3	0.999	1.33	0.0004	159.5	0.996	3.94
Eu(III)	250	36.2	0.038	34.9	0.999	1.61	0.0012	39.7	0.998	1.10
	500	47.0	0.048	45.5	0.999	0.53	0.0013	50.9	0.998	2.01
	750	49.1	0.049	47.4	0.999	1.14	0.0013	52.8	0.999	1.25
	1000	52.4	0.053	49.8	0.998	0.82	0.0013	55.5	0.999	0.92

- In binary systems, both Ce(III) and Eu(III) compete with each other for carbonate ions from crab shell. As a result, decreased biosorptional uptake of Ce(III) and Eu(III) was observed, compared to their respective single component systems. Binary biosorption isotherms were modeled using the extended Langmuir equation with constant interaction factor and the SRS equation. The extended Langmuir equation was not able to predict the experimental data satisfactorily, whereas the SRS equation better predicted the binary isotherms with high correlation coefficients and low % error values.
- Kinetic studies revealed that Ce(III) and Eu(III) biosorption rate was fast for about 96% of Ce(III) and 85% of Eu(III) were removed within 60 min. Among the two kinetic models, viz., pseudo-first and -second order, the pseudo-first order kinetic equation predicted the experimental data accurately with high correlation coefficients and low % error values.
- Overall, this study provides insight into the uptake mechanism and sorption behavior of crab shell for Ce(III) and Eu(III) in single and binary systems.

Acknowledgements

The authors gratefully acknowledge the support and contributions of this project to the Singapore-Delft Water Alliance (SDWA). The research presented in this work was carried out as part of the Singapore-Delft Water Alliance (SDWA)'s research programme (R-264-001-002-272).

References

[1] L.-M. Wang, Q. Lin, L.-J. Yue, L. Liu, F. Guo, F.-M. Wang, Study of application of rare earth elements in advances low alloy steels, J. Alloys Compd. 451 (2008) 534–537.

[2] C. Xu., X. Ai, C. Huang, Research and development of rare-earth cemented carbides, Int. J. Refract. Met. Hard Mater. 19 (2001) 159–168.

[3] T. Liang, S. Ding, W. Song, Z. Chong, C. Zhang, H. Li, A review of fractionations of rare earth elements in plants, J. Rare Earths 26 (2008) 7–15.

[4] J.G. Rabatin, Rare earth X-ray phosphors for medicinal radiography, in: K.A. Gschneidner Jr. (Ed.), Industrial Applications of Rare Earth Elements, American Chemical Society, Washington, DC, 1981, pp. 203–218.

[5] H. Hidaka, A. Masuda, Nuclide analyses of rare earth elements of the Oklo uranium ore samples: a new method to estimate the neutron fluence, Earth Planet. Sci. Lett. 88 (1988) 330–336.

[6] D.W. Bruce, B.E. Hietbrink, K.P. DuBois, The acute mammalian toxicity of rare earth nitrates and oxides, Toxicol. Appl. Pharmacol. 5 (1963) 750–759.

[7] P. Tai, Q. Zhao, D. Su, P. Li, F. Stagnitti, Biological toxicity of lanthanide elements on algae, Chemosphere 80 (2010) 1031–1035.

[8] B. Volesky, Z.R. Holan, Biosorption of heavy metals, Biotechnol. Prog. 11 (1995) 235–250.

[9] K. Vijayaraghavan, Y.-S. Yun, Bacterial biosorbents and biosorption, Biotech. Adv. 26 (2008) 266–291.

[10] T.A. Davis, B. Volesky, A. Mucci, A review of the biochemistry of heavy metal biosorption by brown algae, Water Res. 37 (2003) 4311–4330.

[11] M.Y. Lee, S.H. Lee, H.J. Shin, T. Kajiuchi, J.W. Yang, Characteristics of lead removal by crab shell particles, Proc. Biochem. 33 (1998) 749–753.

[12] J.R. Evans, W.G. Davids, J.D. MacRae, A. Amirbahman, Kinetics of cadmium uptake by chitosan-based crab shells, Water Res. 36 (2002) 3219–3226.

[13] H.C. Niu, B. Volesky, Biosorption of chromate and vanadate species with waste crab shells, Hydrometallurgy 84 (2006) 28–36.

[14] K. Vijayaraghavan, K. Palanivelu, M. Velan, Biosorption of copper(II) and cobalt(II) from aqueous solutions by crab shell particles, Bioresour. Technol. 97 (2006) 1411–1419.

[15] K. Vijayaraghavan, J. Jegan, K. Palanivelu, M. Velan, Removal of nickel(II) ions from aqueous solution using crab shell particles in a packed bed up-flow column, J. Hazard. Mater. B113 (2004) 223–230.

[16] S. Lu, S.W. Gibb, E. Cochrane, Effective removal of zinc ions from aqueous solutions using crab carapace biosorbent, J. Hazard. Mater. 149 (2007) 208–217.

[17] K. Vijayaraghavan, M. Arun, U.M. Joshi, R. Balasubramanian, Biosorption of As(V) onto the shells of the crab (*Portunus sanguinolentus*): equilibrium and kinetic studies, Ind. Eng. Chem. Res. 48 (2009) 3589–3594.

[18] B. Coqblin, Rare earths and actinides, J. Magn. Magn. Mater. 29 (1982) 1–3.

[19] G.N. Sauvion, G.N. Ducros, Catalysis: a growing market for rare earths, J. Less-Common Met. 111 (1985) 23–35.

[20] V. Diniz, B. Volesky, Biosorption of La, Eu and Yb using *Sargassum* biomass, Water Res. 35 (2005) 239–247.

[21] Ş. Sert, C. Kutahyali, S. Inan, Z. Talip, B. Cetinkaya, M. Eral, Biosorption of lanthanum and cerium from aqueous solutions by *Platanus orientalis* leaf powder, Hydrometallurgy 90 (2008) 13–18.

[22] K. Vijayaraghavan, J.R. Jegan, K. Palanivelu, M. Velan, Nickel recovery from aqueous solution using crab shell particles, Adsorpt. Sci. Technol. 23 (2005) (2005) 303–311.

[23] M. Sudhakar, K. Manivannan, P. Soundrapandian, Nutritive value of hard and soft shell crabs of *Portunus sanguinolentus* (Herbst), Int. J. Anim. Veter. Adv. 1 (2009) 44–48.

[24] M.-T. Yen, J.-H. Yang, J.-L. Mau, Physicochemical characterization of chitin and chitosan from crab shells, Carbohydr. Polym. 75 (2009) 15–21.

[25] I. Langmuir, The adsorption of gases on plane surfaces of glass, mica and platinum, J. Am. Chem. Soc. 40 (1918) 1361–1403.

[26] H. Freundlich, Ueber die adsorption in loesungen, Z. Phys. Chem. 57 (1907) 385–470.

[27] O. Redlich, D.L. Peterson, A useful adsorption isotherm, J. Phys. Chem. 63 (1959) 1024.

[28] R. Sips, On the structure of a catalyst surface, J. Chem. Phys. 16 (1948) 490–495.

[29] G. McKay, B. Al-Duri, Simplified model for the equilibrium adsorption of dyes from mixtures using activated carbon, Chem. Eng. Proc. 22 (1987) 145–156.

[30] K.K.H. Choy, J.F. Porter, G. McKay, Langmuir isotherm models applied to the multicomponent sorption of acid dyes from effluent onto activated carbon, J. Chem. Eng. Data 45 (2000) 575–584.

[31] C. Sheindorf, M. Rebhun, M.A. Sheintuch, Freundlich type multicomponent isotherm, J. Colloid Interface Sci. 79 (1981) 136–142.

[32] V.P. Vinod, T.S. Anirudhan, Adsorption behavior of basic dyes on the humic acid immobilized pillared clay, Water Air Soil Pollut. 150 (2003) 193–217.

[33] S. Lagergren, Zur theorie der sogenannten adsorption gelöster stoffe, K. Sven. Vetenskapsakad. Handl. 24 (1898) 1–39.

[34] Y.S. Ho, G. McKay, Pseudo-second order model for sorption processes, Proc. Biochem. 34 (1999) 451–465.

[35] D.S. Kim, B.Y. Park, Effects on the removal of Pb^{2+} from aqueous solution by crab shell, J. Chem. Technol. Biotechnol. 76 (2001) 1179–1184.

[36] V.L. Snoeyink, D. Jenkins, Water Chemistry, John Wiley and Sons, 1980.

[37] M.-Y. Lee, K.-J. Hong, T. Kajiuchi, J.-W. Yang, Determination of the efficiency and removal mechanism of cobalt by crab shell particles, J. Chem. Technol. Biotechnol. 79 (2004) 1388–1394.

[38] R.H. Byrne, E.R. Sholkovitz, in: K.A. Gschneidner Jr., L.R. Eyring (Eds.), Handbook on the Physics and Chemistry of Rare Earths, vol. 23, Elsevier, Amsterdam, 1996, pp. 497–593.

[39] E. Kusaka, Y. Kamata, Y. Fukunaka, Y. Nakahiro, Effect of hydrolyzed metal cations on the liquid–liquid extraction of silica fines with cetyltrimethylammonium chloride, Colloids Surf. 139 (1998) 155–162.

[40] O. Pourret, M. Davranche, G. Gruau, A. Dia, Competition between humic acid and carbonates for rare earth elements complexation, J. Colloids Interface Sci. 305 (2007) 25–31.

[41] G. Crini, Recent developments in polysaccharide-based materials used as adsorbents in wastewater treatment, Prog. Polym. Sci. 30 (2005) 38–70.

[42] C. Kutahyali, S. Sert, B. Cetinkaya, S. Inan, M. Eral, Factors affecting lanthanum and cerium biosorption on *Pinus brutia* leaf powder, Sep. Sci. Technol. 45 (2010) 1456–1462.

[43] A.C. Texier, Y. Andrès, P.L. Cloirec, Selective biosorption of lanthanide (La, Eu) ions by *Mycobacterium smegmatis*, Environ. Technol. 18 (1997) 835–841.

[44] A.C. Texier, Y. Andrs, P.L. Cloirec, Selective biosorption of lanthanide (La, Eu, Yb) by *Pseudomonas aeruginosa*, Environ. Sci. Technol. 33 (1999) 489–495.

[45] R.S. Bai, T.E. Abraham, Studies on chromium(VI) adsorption–desorption using immobilized fungal biomass, Bioresour. Technol. 87 (2003) 17–26.

[46] G. Limousin, J.P. Gaudet, L. Charlet, S. Szenknect, V. Barthes, M. Krimissa, Sorption isotherms: a review on physical bases, modeling and measurement, Appl. Geochem. 22 (2007) 249–275.

[47] R.-S. Juang, H.-J. Shao, Effect of pH on competitive adsorption of Cu(II), Ni(II) and Zn(II) from water onto chitosan beads, Adsorption 8 (2002) 71–78.

[48] K. Vijayaraghavan, S.W. Won, Y.-S. Yun, Single- and dual-component biosorption of reactive black 5 and reactive orange 16 onto polysulfone-immobilized esterified *Corynebacterium glutamicum*, Ind. Eng. Chem. Res. 47 (2008) 3179–3185.